Journal of Industrial and Management Optimization

https://www.aimspress.com/journal/jimo

JIMO, 22(6): 2817–2842.
DOI:10.3934/jimo.2026103
Received: 07 February 2026
Revised: 15 May 2026
Accepted: 19 May 2026
Published: 21 May 2026

Research article

Bayesian risk quantification for power battery closed-loop supply chain network design considering regional heterogeneity

Weiwei Xu[1,2] **and Lipu Zhang**[3,4,*]

[1] Zhejiang Institute of Social Governance and Communication Innovation, Communication University of Zhejiang, Hangzhou 310018, China

[2] School of Cultural Creativity and Management, Communication University of Zhejiang, Hangzhou 310018, China

[3] School of Media Engineering, Communication University of Zhejiang, Hangzhou 310018, China

[4] Key Lab of Film and TV Media Technology of Zhejiang Province, Hangzhou 310018, China

* **Correspondence:** Email: zhanglipu@cuz.edu.cn.

Abstract: The rapid surge in retired power batteries poses a critical challenge for designing cost-efficient and regionally adaptable closed-loop supply chain (CLSC) networks. This study developed a mixed-integer linear programming (MILP) model for a recycling network covering fifty major Chinese cities. The model introduces several novel decision and constraint structures, including differentiated spatial coverage constraints with regional reverse logistics radii (600 km in eastern regions and 1200 km in northwestern areas), a mandatory regional coverage constraint to ensure hub deployment in remote regions, and a conservative demand coverage constraint ensuring feasibility under a bounded 20% demand deviation. A carbon emission penalty term was embedded in the objective function via an auxiliary excess-emission variable linked to a quota allowance. Bayesian inference was used as a post-optimization risk quantification tool to evaluate cost uncertainty due to recovery-rate variability. Our results indicated a baseline system cost of 878 million CNY, driven primarily by forward logistics and facility investments, with limited structural impact from current carbon policies. Bayesian analysis yielded a 7.89 million CNY risk premium for recovery-rate uncertainty. Sensitivity analysis identified critical thresholds triggering network reconfiguration. The framework supports resilient CLSC design under regional and parametric uncertainty.

Keywords: power battery closed-loop supply chain; Bayesian risk quantification; network design; regional heterogeneity; optimization under uncertainty
Mathematics Subject Classification: 90B06, 90C11, 90C15, 62F15, 68U20

1. Introduction

The rapid expansion of electric vehicles (EVs) has accelerated the global transition toward low-carbon transportation systems. However, the large-scale deployment of EVs has simultaneously generated a surge in retired power batteries, posing severe challenges in resource sustainability, environmental protection, and supply chain coordination. As hazardous products with limited life cycles, power batteries require systematic recycling, remanufacturing, and disposal mechanisms. Consequently, CLSC management has emerged as a critical paradigm for integrating forward distribution and reverse recovery activities within a unified optimization framework.

Existing research on EV battery CLSCs has progressed along both methodological and application-oriented directions. On the methodological side, recent advances in CLSC network design and redesign have attracted growing attention. Fathollahi-Fard et al. developed an integrated decision-making framework for CLSC network redesign problems [1], extended the approach to industry-specific contexts such as the tire industry [2], and advanced solution methodologies through adaptive large neighborhood search algorithms with capacity configuration decisions [3] and Lagrangian relaxation reformulations for multi-objective problems under uncertainty [4]. These studies demonstrate the increasing maturity of CLSC network optimization methods and provide a useful foundation for the present work. From a sustainability perspective, multi-objective models have been developed to balance cost, carbon emissions, and recycling performance [5], while hierarchical cost-sharing contracts and carbon policies have been incorporated into CLSC decision structures [6]. Dynamic sustainable business models have been used to evaluate long-term value creation across repurposing and closed-loop recycling modes [7]. Government interventions and regulatory policies have been widely studied, including subsidy mechanisms [8], carbon tax and green incentives [9], stock-flow simulation of recycling policies [10], and optimization models under cap-and-trade and reward–penalty schemes [11]. On the operational side, game-theoretic models have examined recycling strategies under carbon trading [12], mixed recycling channel structures [13], and blockchain-based traceability [14]. Earlier works further addressed collection strategies [15], financial constraints [16], multi-channel competition [17], and material recovery technologies [18].

In addition to the above studies, a growing body of research has formulated MILP models specifically for CLSC network design. Early works by Salema et al. [19] and Zhang et al. [20] established foundational MILP frameworks for integrated forward–reverse network design. Subsequent studies extended these models to multi-period planning under demand uncertainty [21], carbon-aware network design with transport mode selection [22], and robust optimization under demand and facility disruption risks [23]. More recent works have incorporated sustainable objectives into robust CLSC optimization with product family considerations [24], policy-driven green network design under various carbon regulations [25], fuzzy multi-objective formulations for battery industry applications [26], and green CLSC design with emission limits and penalty mechanisms [27].

Despite this progress, several challenges remain for practical EV battery CLSC network design. First, most existing studies emphasize economic-environmental trade-offs, policy incentives, or game-theoretic coordination, whereas integrated network optimization models that simultaneously capture demand uncertainty, carbon regulation, and regional heterogeneity are still limited. Second, the coupling between uncertain demand, reverse logistics capacity planning, and network robustness has not been sufficiently quantified. Third, uncertainty assessment in CLSC planning often relies on

worst-case scenario assumptions, which may lead to overly conservative cost estimates and inefficient budgeting decisions. Motivated by these gaps, this study develops an integrated optimization framework for EV battery CLSC network design. The proposed model incorporates multi-tier logistics structures, carbon emission constraints, and uncertainty characterization within a unified MILP architecture. Through numerical experiments and scenario-based analysis, the model evaluates cost efficiency, recycling performance, and network robustness under alternative policy and market environments. Furthermore, a two-stage Bayesian sampling framework is developed to quantify cost uncertainty induced by recycling-rate variability, providing probabilistic cost estimates that complement conservative worst-case scenario analysis.

The main contributions of this work are summarized as follows. First, a comprehensive CLSC network optimization model is formulated by jointly considering forward distribution and reverse recovery flows under regionally differentiated spatial coverage constraints. Second, carbon regulatory mechanisms and recycling capacity constraints are embedded into the decision structure, enabling quantitative assessment of policy impacts. Third, a conservative demand coverage constraint is incorporated to enhance robustness under bounded demand deviations. Fourth, a two-stage Bayesian sampling framework is developed to quantify cost uncertainty induced by recycling-rate variability and to provide posterior risk estimates for budgeting decisions. Finally, managerial insights are derived to support sustainable battery recycling system design under regional and parametric uncertainty.

Table 1. Comparison of representative CLSC network design models. ND denotes network design. MP denotes multi-period. Cov. denotes spatial coverage constraints. CT denotes cap-and-trade.

Study	MILP	ND	Unc.	Carbon	Cov.	MP	MProd	Key Feature
[19]	✓	✓	–	–	–	△	✓	Integrated strategic–tactical CLSC design
[20]	✓	✓	–	–	–	–	✓	Basic CLSC network optimization model
[21]	✓	✓	Stoch.	Emis. cost	–	✓	✓	Multi-period stochastic CLSC planning
[22]	✓	✓	Det.	Tax/CT	–	✓	✓	Carbon-aware CLSC with transport mode selection
[23]	✓	✓	Robust	–	–	✓	✓	Demand uncertainty + facility disruption robustness
[24]	✓	✓	Robust	Emis. obj.	–	–	✓	Sustainable robust CLSC with product families
[25]	✓	△	–	Policy	–	–	✓	Policy-driven green CLSC under COVID-19
[26]	–	✓	Fuzzy	Emis. obj.	–	–	✓	Fuzzy multi-objective CLSC for the battery industry
[27]	△	✓	Det.	Tax + pen.	–	–	✓	Green CLSC with emission limit and penalty
This study	✓	✓	Bounded + Bayes	Quota + pen.	Reg.	✓	✓	Region-dependent radius + mandatory coverage + Bayesian risk premium

Table 1 summarizes the key features of representative CLSC network design models and highlights the distinctive contributions of this study.

As shown in Table 1, while existing MILP-based CLSC models have made important contributions to network design, few have simultaneously addressed regional heterogeneity in logistics constraints, carbon emission quota mechanisms, and Bayesian-informed uncertainty quantification within a unified framework.

The remainder of the paper is organized as follows. Section 2 presents the model formulation and parameter calibration. Section 3 describes the data sources. Section 4 reports baseline and sensitivity results. Section 5 develops the integrated uncertainty framework. Section 6 concludes the study.

2. Mathematical model

This study develops a MILP model to characterize the optimal configuration of a power battery CLSC network across 50 major consumption cities in China under the joint influence of carbon emission trading regulation and market demand uncertainty. By simultaneously optimizing facility location decisions and logistics flow allocations, the model aims to minimize the overall system cost, which explicitly incorporates quota-plus-penalty expenditures.

2.1. Modeling framework and assumptions

The power battery CLSC network constitutes an integrated circular system composed of forward logistics, connecting manufacturing plants to consumption markets, and reverse logistics, governing the collection and transportation of retired batteries to recycling hubs.

2.1.1. Modeling framework

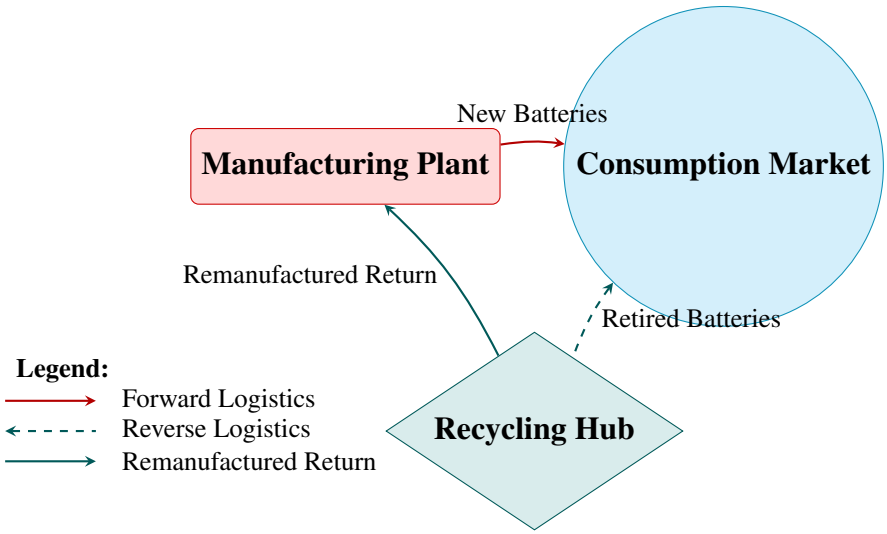

Figure 1. Conceptual physical network structure of the power battery CLSC. Red arrows denote forward logistics (new battery distribution), teal dashed arrows denote reverse logistics (retired battery collection), and the bottom solid teal arrow represents remanufactured material return.

The conceptual physical network structure is illustrated in Figure 1.

As depicted in Figure 1, the CLSC network operates as a closed-loop system where manufacturing plants distribute new batteries to consumption markets through forward logistics, while retired batteries are collected from markets and transported to recycling hubs through reverse logistics. The remanufactured materials are then returned to the production cycle, completing the loop.

2.1.2. Model assumptions

To characterize the operational constraints and regulatory contexts of the new energy vehicles (NEV) power battery recycling network, this study establishes the following core assumptions, which are grounded in industry practices and domestic policy requirements.

Assumption 1 (Demand uncertainty modeling) Demand uncertainty is addressed through a conservative scenario-based approach. Given the pronounced fluctuations observed in annual power battery sales, the maximum demand deviation is calibrated as 20% of the baseline market demand. Accordingly, the peak-demand scenario is defined as

$$D^{\mathrm{p}} = D^0(1 + 0.2\gamma),$$

where D^0 denotes the baseline demand and γ is a deviation scaling factor. To guarantee network resilience under extreme conditions, we enforce demand satisfaction under the worst-case realization by setting $\gamma = 1.0$.

It should be noted that this formulation adopts a deterministic worst-case boundary scenario rather than a formal robust optimization framework with a controlled budget of uncertainty. This choice is motivated by the need to ensure full service capability under the most demanding realization, prioritizing operational safety over the conservatism–cost trade-off typically encountered in adjustable robust optimization.

Assumption 2 (facility capacity constraints) Differentiated capacity rules are imposed on forward and reverse logistics nodes:

- *Forward logistics*: Manufacturing plants are assumed to possess sufficient production capacity to meet all market demand, hence no binding output constraints are imposed on the forward supply chain.
- *Reverse logistics*: Recycling hubs are constrained by technological processing limits and site scale. The maximum annual treatment capacity of each hub is calibrated at 80,000 standard battery units, reflecting realistic bottlenecks in commercial recycling infrastructure in China.

Assumption 3 (carbon emission and regulatory mechanism) Transport-related carbon emissions are modeled with directional heterogeneity, and carbon regulation follows a baseline quota mechanism:

- Unit emission factors are differentiated by logistics direction. Due to gaps in loading efficiency, packaging standards, and hazardous material handling requirements between new and retired batteries, distinct factors β_1 (forward logistics) and β_2 (reverse logistics) are adopted.

- A quota-plus-penalty mechanism is imposed only on the part of annual total emissions that exceed the mandatory baseline quota C. Intertemporal quota banking and cross-enterprise carbon trading are not incorporated in the baseline model.

Assumption 4 (spatially differentiated accessibility rules) To accommodate China's vast territorial scale and uneven regional development, the model introduces geographically heterogeneous reverse logistics coverage constraints:

- For densely populated central and eastern regions, the maximum economically viable reverse logistics service radius is set at 600 km; transportation beyond this threshold is prohibited.
- For sparsely populated northwestern regions (e.g., Urumqi, Xi'an), the uniform 600 km standard would result in network coverage gaps. Hence, the service radius is extended to 1200 km, with a mandatory constraint that at least one recycling hub must be deployed in this region.
- This differentiated design balances the trade-off between elevated transportation costs and the strategic requirement for full network accessibility and structural completeness in remote areas.

2.1.3. Methodological justification

The MILP framework is selected based on the structural characteristics of the CLSC network design problem. First, the decision structure inherently combines discrete and continuous variables: facility location decisions are binary (a hub is either selected or not), while logistics flows and capacity utilizations are continuous quantities—a hybrid structure that MILP accommodates natively. Second, the core cost and constraint relationships (transportation costs proportional to distance and flow, linear carbon penalties, capacity and coverage constraints) are naturally linear, making MILP an exact representation rather than a simplifying approximation.

Compared to alternative approaches, MILP offers distinct advantages for this problem. Heuristic and meta-heuristic methods cannot guarantee global optimality, which is critical when solutions inform multi-million CNY infrastructure investments. Nonlinear formulations (NLP/MINLP) would add computational complexity without substantive gains given the linear nature of the underlying relationships. Stochastic programming requires explicit probability distributions that are often unavailable in emerging industries such as power battery recycling. Simulation-based methods are computationally prohibitive for scenario analysis, while game-theoretic models, widely used for decentralized multi-agent competition, are less suitable for centralized network design under a unified decision-maker. The MILP framework thus ensures globally optimal solutions, computational tractability at practical scale, and transparent, interpretable results.

2.2. Sets, parameters, and decision variables

To clearly define the structural elements and quantitative boundaries of the proposed optimization model, the notation system is organized into three categories: sets, parameters, and decision variables.

2.2.1. Set definitions

The core decision entities and geographical scope involved in the network are defined as follows:

- $i \in F$: Set of manufacturing plants, with $|F| = 6$, including Xi'an, Changsha, Shenzhen, Shanghai, Chengdu, and Beijing;
- $j \in M$: Set of consumption markets, with $|M| = 50$, covering major national demand cities from Chengdu and Hangzhou to Jiaxing;
- $k \in R$: Set of candidate recycling hubs, with $|R| = 22$, located in logistics nodes such as Zhengzhou, Hefei, and Urumqi;
- $R_{NW} \subseteq R$ and $M_{NW} \subseteq M$: Subsets of recycling hubs and consumption markets located in northwestern regions, defined as $R_{NW} = M_{NW} = \{\text{Urumqi}, \text{Xi'an}\}$, introduced to enforce the extended 1200-km reverse logistics service radius for geographically dispersed areas.

2.2.2. Parameter definitions

The model parameters span multiple structural dimensions, including demand characteristics, cost structures, environmental impacts, regulatory policies, and operational constraints. All parameter values are calibrated based on industry statistics and policy documents from 2024–2025. Detailed definitions are summarized in Table 2.

Table 2. Parameter definitions of the power battery CLSC model.

Symbol	Description
c_{ij}, c_{jk}	Unit transportation cost between nodes (CNY)
d_j	Baseline retired battery demand in market j (units)
u_j	Demand uncertainty deviation
f_k	Fixed establishment and admission cost of recycling hub k
t	Transportation cost coefficient per unit distance and flow
d_{ab}	Spatial distance between node a and node b
α	Statutory battery recovery rate target
β_1, β_2	Carbon emission factors for forward and reverse transportation
C	Annual free carbon emission allowance
τ	Penalty price
q_k	Maximum annual processing capacity of recycling hub k
$d^{\max}$	Maximum economic service radius of reverse logistics (regular regions)
d^{nw}	Maximum reverse logistics radius in northwestern regions
γ	Deviation scaling factor for demand uncertainty

2.2.3. Decision variables

The core optimization decisions of the proposed model are implemented through the following variables, which jointly characterize flow allocation and facility location planning within the CLSC network:

- $x_{ij} \geq 0$: quantity of forward product flow shipped from plant i to market j;
- $z_{jk} \geq 0$: volume of retired batteries transported from market j to recycling center k;
- $y_k \in \{0, 1\}$: binary facility location variable indicating whether recycling center k is established;
- $e_e \geq 0$: auxiliary variable representing the amount of carbon emissions exceeding the allocated cap.

2.3. Model formulation

The network configuration problem of the power battery CLSC is formulated as a MILP model. The objective is to minimize the total system cost, including economic expenditures and environmental penalty costs, while satisfying market demand, regulatory requirements, and operational constraints. The objective function Z is defined as follows:

$$\min Z = \sum_{k \in R} f_k y_k + \sum_{i \in F} \sum_{j \in M} c_{ij} x_{ij} + \sum_{j \in M} \sum_{k \in R} c_{jk} z_{jk} + \tau \cdot e_e \tag{2.1}$$

The objective function consists of four components: fixed establishment and operation costs of recycling centers, forward transportation costs, reverse logistics transportation costs, and penalties imposed on emissions exceeding the allocated quota. Unit transportation costs are distance-proportional, defined as $c_{ij} = d_{ij} \times t$ and $c_{jk} = d_{jk} \times t$.

To ensure physical feasibility and regulatory compliance, the optimization is subject to the following constraints.

First, to address market uncertainty, a conservative demand coverage constraint is imposed. Forward shipments must satisfy worst-case demand considering fluctuation factor γ, where $u_j = 0.2 \times d_j$ denotes demand variability:

$$\sum_{i \in F} x_{ij} \geq d_j + \gamma \cdot u_j, \quad \forall j \in M \tag{2.2}$$

Second, reverse flows must comply with extended producer responsibility regulations. A minimum recovery rate α is enforced to ensure that collected retired batteries from each market meet statutory targets:

$$\sum_{k \in R} z_{jk} \geq d_j \cdot \alpha, \quad \forall j \in M \tag{2.3}$$

Facility capacity constraints are incorporated through logical linking relationships. Reverse flows can only be allocated to established facilities, and total inflow cannot exceed annual processing capacity q_k:

$$\sum_{j \in M} z_{jk} \leq q_k \cdot y_k, \quad \forall k \in R \tag{2.4}$$

To internalize environmental externalities, a quota-plus-penalty carbon constraint is introduced. Total emissions are calculated with differentiated emission factors for forward and reverse logistics.

Any emissions exceeding the allocated quota C are defined as excess emissions:

$$\left(\sum_{i\in F}\sum_{j\in M}\beta_1\, d_{ij}\, x_{ij} + \sum_{j\in M}\sum_{k\in R}\beta_2\, d_{jk}\, z_{jk}\right) - C \le e_e \tag{2.5}$$

To reflect spatial heterogeneity, differentiated geographic service radius constraints are imposed. For densely populated eastern regions, the conventional economic service radius is set to $d^{\max} = 600$ km. For sparsely populated northwestern regions (M_{NW} and R_{NW}), the radius is relaxed to $d^{\mathrm{nw}} = 1200$ km:

$$z_{jk} = 0, \quad \text{if } \begin{cases} d_{jk} > d^{\mathrm{nw}}, & \text{if } j \in M_{NW} \text{ or } k \in R_{NW} \\ d_{jk} > d^{\max}, & \text{otherwise} \end{cases} \tag{2.6}$$

To complement the distance relaxation strategy, a regional coverage constraint is enforced. At least one recycling facility must be established within the northwestern subset R_{NW} to ensure service accessibility:

$$\sum_{k\in R_{NW}} y_k \ge 1 \tag{2.7}$$

Finally, non-negativity and binary restrictions on decision variables are defined as:

$$x_{ij},\, z_{jk},\, e_e \ge 0; \quad y_k \in \{0, 1\} \tag{2.8}$$

3. Data sources and parameter calibration

The case study covers fifty major consumption cities across China, with six manufacturing plants and twenty-two candidate recycling hubs forming the candidate node set. The geographic distribution of all network nodes is visually presented in Figure 2 (Section 4.1.2), which displays the final optimized layout.

3.1. NEV sales and demand calibration

The 2024 NEV sales in major Chinese cities were used to calibrate urban demand. Three primary sources were considered: the China Automotive Data Research Institute report on NEV sales, the 2025 national forecast of retired power battery volume (0.82 million tons), and the China Association of Automobile Manufacturers' 2024 production statistics.

To quantify demand for optimization, city-level demand is allocated proportionally to NEV sales. A standardized battery pack unit is adopted, with one unit representing approximately 0.5 tons of retired batteries. This benchmark acts as a normalization factor: rescaling the absolute demand of each city preserves the inter-city demand ratios, ensuring model validity.

The processed city-level demand data are summarized in Table 3. Sources and references are listed in the table notes.

Table 3. NEV sales and calibrated demand in major cities (2024).

City	Sales (10^4 units)	Demand (units)	City	Sales (10^4 units)	Demand (units)
Chengdu	30.97	39,500	Shijiazhuang	12.34	15,700
Hangzhou	30.76	39,200	Jinan	12.16	15,500
Shenzhen	30.09	38,400	Foshan	12.03	15,300
Shanghai	29.74	37,900	Qingdao	11.90	15,200
Beijing	29.08	37,100	Changchun	11.63	14,800
Guangzhou	27.70	35,300	Shenyang	11.32	14,400
Zhengzhou	23.74	30,300	Nanning	10.51	13,400
Chongqing	22.67	28,900	Taiyuan	9.84	12,500
Xi'an	22.57	28,800	Kunming	9.66	12,300
Tianjin	22.52	28,700	Linyi	9.53	12,100
Wuhan	22.04	28,100	Taizhou	9.16	11,700
Suzhou	21.93	28,000	Jinhua	9.07	11,500
Hefei	16.66	21,200	Xuzhou	8.83	11,200
Wuxi	15.31	19,500	Haikou	8.60	10,900
Ningbo	15.28	19,500	Jining	8.34	10,600
Dongguan	14.47	18,400	Xiamen	8.12	10,300
Nanjing	14.37	18,300	Baoding	8.06	10,200
Changsha	13.84	17,600	Nanchang	7.64	9700
Wenzhou	13.64	17,300	Changzhou	7.56	9600
Guiyang	7.33	9300	Weifang	6.66	8500
Luoyang	7.28	9200	Urumqi	6.49	8200
Tangshan	6.84	8700	Quanzhou	6.46	8200
Nantong	6.81	8700	Fuzhou	6.36	8100
Harbin	6.75	8600	Zhongshan	6.14	7800
Handan	6.72	8500	Jiaxing	6.11	7800

[a] Taking Chengdu as an example, the demand unit is calculated as $\frac{0.82 \text{ million tons}}{0.5 \text{ tons/unit}} \times \frac{4.0374 \text{ million}}{12.866 \text{ million}} \times \frac{0.3097 \text{ million}}{4.0374 \text{ million}}$, which is normalized to 39,500 units.

[b] Data sources: CADRI 2024 NEV sales, Luo 2025 retired battery forecast, CAAM 2024 NEV production.

3.2. Calibration of fixed cost and processing capacity parameters

The fixed construction cost of power battery recycling centers and the processing capacity of individual facilities constitute key economic parameters that determine the network configuration. The data employed in this study are primarily compiled from the Ministry of Industry and Information Technology (MIIT) white-list enterprise announcements, EVTank industry white papers, and publicly disclosed investment information of leading firms (e.g., GEM, Brunp, Jereh Environmental), including Environmental Impact Assessment (EIA) reports, prospectuses, and annual reports.

Table 4 presents the calibration process and adopted values of fixed costs for candidate hub locations. It should be emphasized that the fixed cost parameter f_k in the model does not represent the total project investment. Instead, it denotes the annualized fixed cost obtained through dual adjustments of core production line investment allocation and annual depreciation amortization. The

calculation is formulated as follows:

$$f_k = \frac{I_t \times \eta_c \times (1 - r)}{T} + C_m \tag{3.1}$$

where I_t denotes the total project investment, η_c represents the investment share of core recycling production lines (typically ranging from 25% to 40%), r is the residual value rate (set at 5%), T is the depreciation period (assumed to be 10 years), and C_m denotes the annual facility-specific maintenance and operation cost.

This treatment ensures that the magnitude of fixed costs is commensurate with annual transportation and operating costs, thereby avoiding optimization bias caused by dimensional inconsistency.

Table 4. Calibration of fixed construction cost parameters for power battery recycling centers (2024–2025).

Param. Type	Ref. Project (Company)	Inv. (Bn CNY)	Val. (10k CNY)	Calculation Logic & Data Source
Hefei-type	Rongjie Power	17.4	5800	Core production line investment approx. 580 million CNY.
Zhengzhou-type	Jerry Env.	10.2	5300	Converted from 100,000 ton annual capacity.
Guiyang-type	Guizhou Red Star	4.3	5000	Single-factory dedicated recycling project.
Changsha-type	Jinkai Recycling	50.0	6200	Allocation based on 15% share of core production line investment.
Wuhan-type	Ruikemei	5.0	5800	Phase I dry-process recycling project.
Yibin-type	GEM	8.0	7,000	Allocation based on 7:1 proportion.
Nanchang-type	Hengrun New Mat.	15.0	5500	Allocation based on 2:1 investment density.

In addition, the processing capacity parameters of recycling centers are calibrated based on the officially disclosed capacities of enterprises listed in the MIIT "white list" and the industry average operational level, as summarized in Table 5.

Table 5. Processing capacity parameters for recycling centers and data sources.

Indicator	Range (kt/yr)	Value (kt/yr)	Source and Validation Logic
Single-factory	1–5	4	Policy threshold (MIIT): The 2024 industry standards require a minimum of 0.5 kt/yr (recycling) and 0.1 kt/yr (cascade). Policies encourage aggregation. Empirical evidence: Pareto distribution observed (CR10 = 62.3%). Leading firms (GEM, Brunp) target 4–5 kt/factory, aligning with model assumptions.[1,2]
Avg. Capacity of	1–2	-	Statistical adjustment (EVTank): 2023 average capacity of 156 whitelisted firms was 2.43 kt/yr. Corrected to 1–2 kt/yr after excluding outliers (¿4 kt). Logic: Reflects firms meeting compliance (¿0.5 kt) but lacking leading-scale efficiency.[2]

[1] MIIT / Hubei MIIT: Industry Standard Conditions for Power Battery Recycling (2024).

[2] EVTank / Yiwei Research: White Paper on Lithium-ion Battery Recycling Industry in China (2024).

3.3. Transportation cost, carbon emissions, and policy parameters

The logistics and carbon-policy-related parameters involved in this model are primarily calibrated using data from China's national carbon market transactions (2024–2025), hazardous materials logistics industry statistics, and ESG disclosures of leading battery recycling enterprises. The specific parameter values, units, and data sources are summarized in Table 6.

Table 6. Transportation, carbon emission, and policy parameters (2024–2025).

Parameter	Range	Value	Unit[a]	Source and Calculation Logic
Transport Cost	1.2–1.6	1.6	CNY/km	Market quotes: Median long-distance shipping prices for Class 9 hazardous goods (Autohome/PCauto), including compliance costs.[1]
Carbon Factor	-	0.5/1.0 ($\times 10^{-4}$)	tCO_2/km	ZEROLab: Forward (0.5) / Reverse (1.0). Bottom-up calculation using Scope-3 GHG Protocol (well-to-wheel).[2]
Carbon Price	50–82	65	CNY/tCO_2	MEE Report (2024): Based on cumulative trading average (65.6) and core trading range (55–75).[3]
Carbon Allowance	-	16,000	tCO_2	Model calibration: Benchmarked against industry leaders (CATL) and scaled to network size to serve as a binding constraint.[4]
Reverse Radius	300–500	600	km	Operational limit: Based on 72h traceability and 2026 market scale estimates. 600 km is cost-optimal.[5]

[a] Note: The unit denominator implies a standardized battery pack ($\approx$ 0.5 t).
[1] Sources: Autohome, PCauto.
[2] ZEROLab GHG S3.4/3.9 (2024).
[3] MEE National Carbon Market Report (2024).
[4] Allowance calibration: As specific quotas for regional networks are policy-dependent, this value is calibrated using CATL's emission intensity (2023 Sustainability Report) as a reference. It is scaled proportionally to the modeled network's throughput to establish a baseline where carbon constraints are binding, facilitating the analysis of penalty costs. CATL 2023 Carbon Report.
[5] OFweek Forecast (2026).

The statutory recycling rate target coefficient α is set to 28%. This value is chosen as a realistic baseline reflecting the current effective recovery level in China. It is consistent with the MIIT regulatory framework for NEV power-battery recycling, including *Interim Measures for the Management of Recycling and Utilization of Power Batteries for NEVs* (2026) and *Normative Conditions for Comprehensive Utilization of Retired Power Batteries from NEVs (2024 Edition)*, which enforce extended producer responsibility and traceable take-back requirements. Moreover, industry statistics reported in EVTank (2024) and disclosed compliance information from MIIT white-listed enterprises indicate that the formal-channel collection and regulated recycling share remains at a moderate level under current infrastructure constraints. To ensure robustness, α is further examined in the sensitivity range $\alpha \in [0.20, 0.36]$, covering both conservative and enhanced-recovery scenarios.

The selected value not only satisfies the minimum regulatory requirements for closed-loop recovery assurance, but also reflects the current technological feasibility and economic viability of large-scale battery recycling in China. Meanwhile, it reserves a reasonable fluctuation interval for subsequent sensitivity analysis, with $\alpha \in [0.20, 0.36]$.

4. Numerical optimization results

The proposed MILP model was solved using the Python for mathematical programming (PuLP) modeling framework with the COIN branch and cut solver (CBC) [28, 29]. The model integrates geodesic-based distance approximations, unit transportation costs, carbon emission factors for logistics, linear penalties under carbon allowance constraints, and robust demand satisfaction. All key parameters were calibrated based on publicly available data from China's power battery recycling industry in 2025, ensuring the numerical results are interpretable and realistic.

4.1. Baseline scenario optimization results

Based on the optimized CLSC model, this section evaluates performance from three perspectives: economic cost, environmental impact, and network operational efficiency. Results are summarized in Table 7 and Table 8, and are interpreted considering regional characteristics, policy constraints, and supply chain optimization logic.

4.1.1. Numerical results

Table 7. Economic and environmental performance indicators of the CLSC

Indicator	Value	Unit	Share (%)
Economic Performance			
Total Objective Cost	877.58	10^6 CNY	100.00
Fixed Construction Cost	333.00	10^6 CNY	37.95
Forward Logistics Cost	435.85	10^6 CNY	49.67
Reverse Logistics Cost	108.44	10^6 CNY	12.36
Emission Penalty Payment	0.29	10^6 CNY	0.03
Environmental Impact			
Total Carbon Emissions	20.40	10^3 tCO_2	–
Forward Emission Contribution	13.62	10^3 tCO_2	66.77
Reverse Emission Contribution	6.78	10^3 tCO_2	33.23
Network Efficiency			
Average Forward Transport Distance	260.78	km	–
Average Reverse Transport Distance	278.07	km	–

Note: Economic indicators are expressed in million CNY; carbon emissions in thousand tons of CO_2; emission penalty values are rounded to two decimal places for presentation clarity.

Table 7 shows that the total CLSC cost is 877.58 million CNY, with a structure dominated by forward logistics and supplemented by fixed construction investment. Forward logistics accounts for

49.67% of total expenditure, reflecting large-scale transportation from six battery production bases (Xi'an, Shanghai, Shenzhen, etc.) to 50 consumption markets nationwide. High-demand clusters such as the Yangtze River Delta (Hangzhou, Shanghai), Pearl River Delta (Shenzhen, Guangzhou), and Beijing-Tianjin-Hebei regions concentrate most of the demand, while remote northwestern markets (e.g., Urumqi) are supplied from distant factories (Xi'an, Chengdu), driving up forward logistics costs.

Fixed construction costs account for 37.95%, corresponding to the strategic deployment of six recycling centers. This investment balances coverage and cost efficiency: high-capacity hubs in densely populated eastern regions match strong demand, whereas remote northwestern nodes minimize excess fixed cost. Reverse logistics cost is 12.36%, lower than forward logistics, due to the 28% statutory recycling rate limiting transportation scale and regionalized collection reducing distances. It should be emphasized that the baseline cost and hub configuration are directly shaped by the demand uncertainty constraint embedded in the model: this constraint requires the network to satisfy 120% of baseline demand, which not only drives the total system cost to 877.58 million CNY, but also pushes core recycling hubs such as Hangzhou, Tianjin, and Xi'an to high utilization rates.

The emission penalty payment amounts to only 0.29 million CNY, indicating that the carbon allowance of 16,000 tCO_2 effectively covers most supply chain emissions. This result aligns with the design of the carbon constraint under the quota-plus-penalty mechanism: prioritizing short-distance transportation routes and regionalized collection significantly reduces excess emissions and the corresponding penalty burden.

Total CLSC emissions reach 20,400 tCO_2, with forward logistics contributing 66.77% and reverse logistics 33.23%. Despite reverse logistics having a higher emission factor, lower transport volume due to the statutory recycling limit reduces its overall share. This highlights the key role of transportation scale in emission control.

Average forward and reverse transport distances are 260.78 km and 278.07 km, respectively. Longer reverse distances are due to the northwestern hubs (Xi'an, Urumqi) employing a 1200 km service radius to cover sparse regions, avoiding low-utilization facilities that would increase emissions, reflecting a trade-off between regional adaptation and environmental efficiency.

Table 8. Operational performance and capacity utilization of recycling Centers.

Location	Processed Units	Utilization (%)	Fixed Cost (10^6 CNY)
Hangzhou	80,000	100.00	6.00
Tianjin	54,460	68.08	5.70
Xi'an	52,160	65.20	5.60
Shenzhen	44,240	55.30	6.50
Changchun	10,584	13.23	4.80
Urumqi	2296	2.87	4.70
Average	43,957	50.78	5.55

Note: Fixed costs are converted from original data in 100,000 CNY to million CNY; averages are calculated across active hubs.

Table 8 highlights spatial differentiation in hub utilization. Hangzhou operates at full capacity to serve the high-demand Yangtze River Delta (including Shanghai, Suzhou, Ningbo), demonstrating resource concentration in core demand areas and achieving cost and emission minimization via

short-distance coverage. Tianjin (68.08%) and Xi'an (65.20%) serve the Bohai Rim and northwestern markets, leveraging geographic advantage while maintaining high utilization. Shenzhen (55.30%) serves the Pearl River Delta, achieving efficient, clustered logistics.

This significant spatial differentiation in hub utilization is the direct consequence of the regional heterogeneity constraint embedded in the model. For densely populated eastern regions, hubs such as Hangzhou operate at 100% capacity to achieve cost-efficient clustered collection and transport for the high-demand Yangtze River Delta. In contrast, the northwestern hub (Urumqi) operates at only 2.87% utilization, which is not an optimization inefficiency, but a deliberate strategic trade-off between remote region accessibility and local economic efficiency: the model sacrifices partial local economic efficiency to avoid long-distance transport from Xinjiang to central hubs, ensuring network coverage and supply chain resilience in geographically dispersed areas. Average hub utilization is 50.78%, indicating balanced allocation that ensures both core market efficiency and peripheral coverage.

4.1.2. Visualization of results

To better interpret the spatial distribution and operational logic of the optimized network, Figure 2 provides a graphical overview of the 2025 optimal CLSC layout.

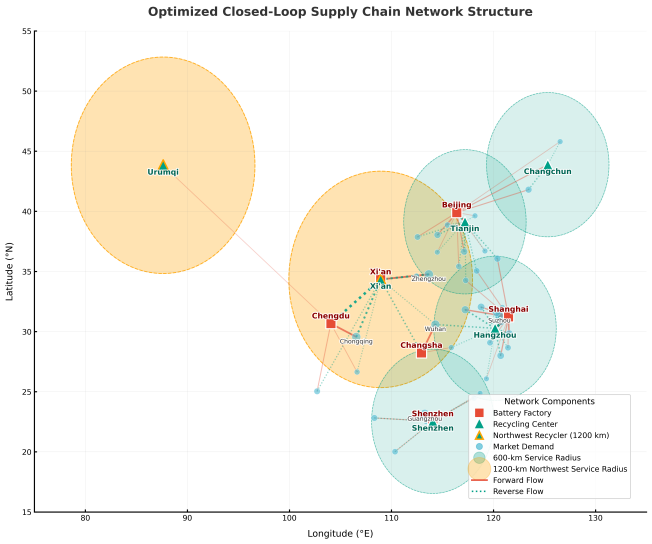

Figure 2. Optimal layout of the 2025 power battery CLSC.

Figure 2 visually depicts the optimized network configuration. Red squares denote six production bases concentrated in core demand regions. Green triangles represent recycling hubs with a dual service radius: a 600-km light-blue circle covers high-demand eastern areas, and a 1200-km light-yellow circle provides strategic coverage in remote northwestern areas. Light-blue circles indicate consumer markets, with size proportional to demand. Red solid lines (forward logistics) and green dashed lines (reverse logistics) illustrate flow volumes. This regionally differentiated layout achieves short-distance efficient logistics in high-demand zones while ensuring network accessibility in remote regions, confirming the model's synergistic optimization of cost, coverage, and operational efficiency.

4.1.3. Complexity analysis

To further evaluate the computational efficiency of the proposed model, we conducted a complexity analysis by generating and solving five instances with increasing numbers of consumption markets (10, 20, 30, 40, and 50). The results, summarized in Table 9 and Figure 3, reveal a distinct nonlinear relationship between problem size and solver performance. While the number of decision variables grows linearly, the CPU time exhibits a pronounced superlinear increase across the tested range of 10–50 markets. Notably, as the network scale increases from 40 to 50 markets, the number of variables increases by approximately 25%, but the solver time surges by nearly 5.7 times. This behavior is consistent with the NP-hard nature of the MILP formulation, indicating that while the exact solver remains highly efficient for the national-scale base case (50 cities), the computational cost will increase significantly for larger network expansions.

Table 9. Computational performance under different network sizes.

Number of Markets	Number of Variables	CPU Time (s)
10	303	0.08
20	583	0.07
30	863	0.22
40	1143	0.28
50 (Base Case)	1423	1.90

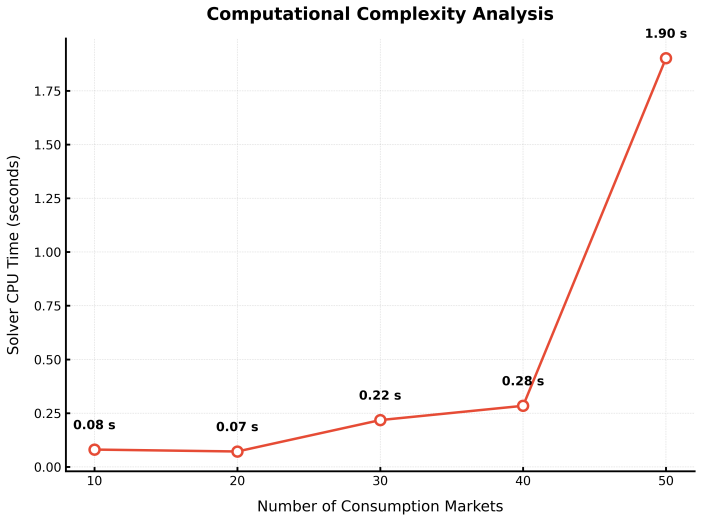

Figure 3. Solver CPU time as a function of problem size. The curve shows a nonlinear increase in computational effort, particularly at the 50-city scale.

4.1.4. Key insights

Three main insights emerge from the performance analysis. First, cost optimization should focus on forward logistics and fixed construction investment. Subsequent reductions are feasible via demand-oriented production base placement and regionalized recycling networks. Second, carbon

allowances effectively constrain supply chain emissions without imposing significant economic burden, confirming feasibility of economic–environmental co-optimization. Third, combining a 1200-km extended service radius in the northwestern with high-utilization eastern hubs balances efficiency and geographic coverage, providing a scalable paradigm for large, spatially heterogeneous supply chains. Overall, the model effectively addresses regional demand heterogeneity, policy constraints, and environmental targets, offering guidance for both industry practice and policymaking.

4.2. Four-factor sensitivity analysis

To examine the structural stability of the CLSC model under multiple institutional and operational constraints, and to quantify the effects of key parameter perturbations on system performance, a single-factor sensitivity analysis is conducted on four core variables: statutory recycling rate, quota-plus-penalty stringency, carbon allowance, and recycling center processing capacity. By systematically varying one parameter while holding the others constant, we analyze its impacts on total system cost, facility deployment, and network operational status, thereby revealing the inherent quantitative mechanisms behind CLSC optimization.

Tables 10 and 11, together with Figure 4, show the effects of core parameters on cost and operational performance. Overall, parameter impacts differ significantly: the statutory recycling rate and recycling center processing capacity dominate cost and network structure, while the quota-plus-penalty mechanism and carbon allowance have minimal regulatory pressure and marginal effects on operational decisions.

Table 10. Key results of single-factor sensitivity analysis for the power battery CLSC.

Parameter	Base Value	Variation Range	Total Cost Change (%)	No. of Recycling Centers	Elasticity	Key Threshold
Statutory Recycling Rate α	0.28	0.20–0.36	−6.28–+5.59	5–6	0.1656–0.2384	0.28 Network configuration threshold
Quota-Plus-Penalty ($CNY \cdot tCO_2^{-1}$)	65	45.5–84.5	−0.01–+0.01	6	3.0×10^{-4}	—
Carbon Allowance (tCO_2)	16,000	12,800–19,200	−0.02–+0.02	6	−0.0012	19,200 Excess emission narrowing
Recycling Center Capacity (units)	80,000	56,000–104,000	−1.16–+4.56	5–7	−0.1520–−0.0041	68,000 Capacity constraint threshold

Table 11. Core operational indicators under the baseline scenario.

Indicator	Value
Total System Cost (10^4 CNY)	87,758.12
Share of Fixed Construction Cost	37.95%
Share of Transportation Cost	62.02%
Share of Quota-Plus-Penalty Payment	0.03%
Total Carbon Emissions (tCO_2)	20,398.06
Excess Carbon Emissions (tCO_2)	4,398.06
Number of Constructed Recycling Centers	6
Core Hub Utilization	Hangzhou 100.00%, Tianjin 68.08%, Xi'an 65.20%
Actual Recycling Rate	28.00% (aligned with the statutory target)

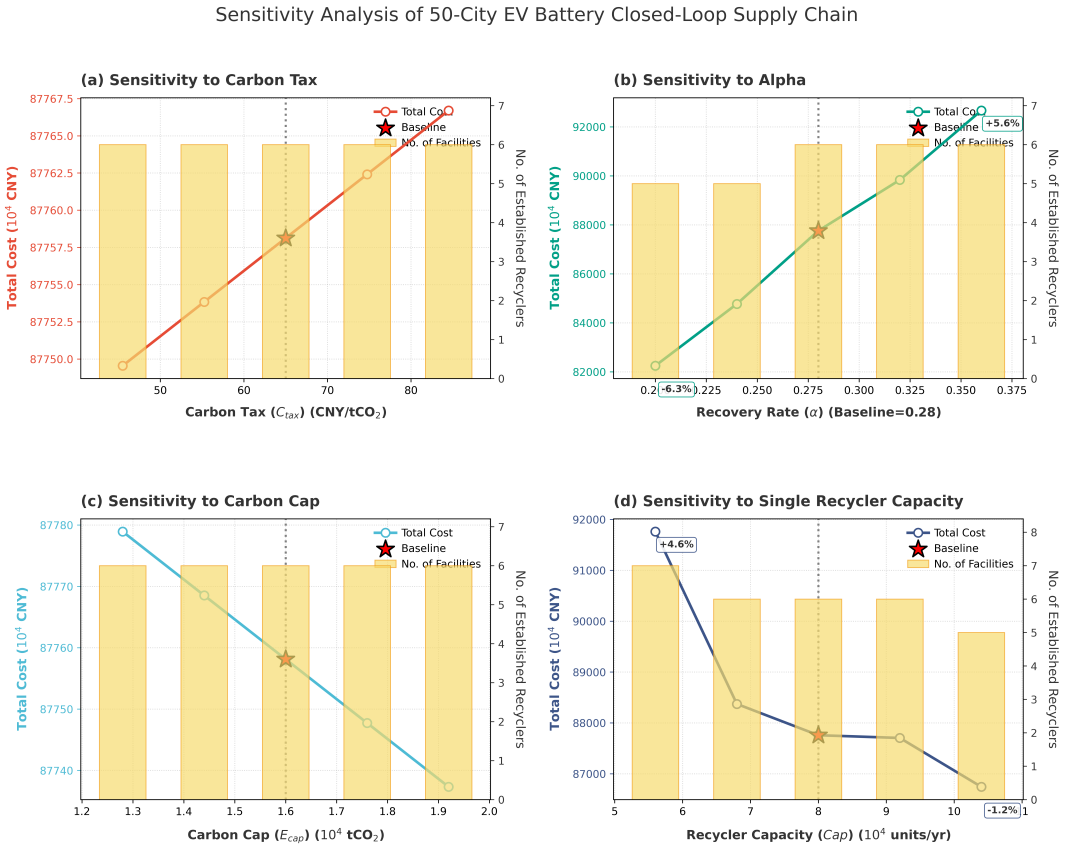

Figure 4. Impact of key parameter variations on total cost (±20% around base values).

Increasing the statutory recycling rate has the most pronounced effect on total cost and network configuration. As α rises from 0.20 to 0.36, total system cost increases from 822.476 million CNY to 926.678 million CNY, a change of $-6.28\% \sim +5.59\%$, with elasticity ranging from 0.1656–0.2384, reflecting typical marginally increasing cost. This is driven by expanded reverse logistics and saturation of core hub processing capacity. Facility response shows that for $\alpha \leq 0.24$, the system can reduce

the number of hubs (6→5) and increase single-hub utilization to absorb demand changes. At α = 0.28 (baseline) and 0.32, six hubs are deployed, with utilization in Hangzhou and Xi'an reaching 100%. At $\alpha = 0.36$, the three core hubs (Hangzhou, Xi'an, Tianjin) approach full capacity, confirming 0.28 as the critical threshold for hub deployment, beyond which utilization rises sharply. Thus, the statutory recycling rate not only affects cost but also shapes network configuration via facility capacity constraints.

In contrast, the quota-plus-penalty mechanism and carbon allowance exert minor cost transmission effects and negligible influence on operational decisions. Increasing the quota-plus-penalty rate from 45.5 to 84.5 CNY·tCO_2^{-1} leads to a total cost change of only $-0.01\% \sim +0.01\%$, with an elasticity around 3×10^{-4}, while hub deployment and facility utilization remain unchanged. Adjusting the carbon allowance within 12,800–19,200 tCO_2 results in cost variations of $-0.02\% \sim +0.02\%$ and an elasticity of -0.0012. Even at the upper limit of 19,200 tCO_2, excess emissions still reach 1,198.06 tCO_2, implying that carbon constraints cannot be fully relaxed. As shown in Table 11, the quota-plus-penalty payment accounts for merely 0.03% of the total system cost, which is too low to reshape hub layout or transportation routes. This further demonstrates the limited regulatory effect of a single carbon constraint instrument.

Recycling center capacity exhibits a threshold-based, bidirectional impact mechanism, directly triggering adjustments in hub number and utilization. Below 68,000 units, the system adds one hub (6→7) to satisfy reverse demand, raising the fixed cost share from 37.95% to 41.96% and the total cost by 4.56%. Between 68,000–92,000 units, demand constraints dominate, the hub count remains 6, and core utilization moderately declines (e.g., Hangzhou 100% → 93.53%). Above 104,000 units, hub number can be reduced (6→5) while scaling single-hub processing, lowering the total cost by 1.16% and fixed cost share to 31.82%. Core hub utilization remains spatially differentiated, with Hangzhou at 100% and Changchun/Urumqi at 13.23%/2.87%, reflecting alignment with regional demand. Carbon emissions are mainly from forward logistics (66.77%), emphasizing its central role in low-carbon optimization.

In summary, the statutory recycling rate and hub processing capacity jointly shape the CLSC cost trajectory and network expansion and contraction patterns. Variations in these parameters trigger dual adjustments in system cost and facility deployment, whereas the quota-plus-penalty mechanism and carbon allowance exert negligible impacts under the baseline cost structure. The identified critical thresholds (recycling rate of 0.28 and hub capacity of 68,000 units) offer quantitative guidance for network expansion scheduling, hub capacity configuration, and the design of synergistic mechanisms between carbon regulation and recycling policies.

5. Integrated analysis of Bayesian inference and worst-case scenario analysis

This section proposes a two-stage framework to quantify the impact of recycling rate uncertainty (α) on CLSC network costs. In Stage 1, Bayesian MCMC sampling is performed to estimate the posterior distribution of α by integrating industry prior knowledge with empirical observations. In Stage 2, posterior samples are propagated through the deterministic MILP model to obtain the induced distribution of total network cost.

It should be emphasized that this procedure does not construct a fully integrated stochastic programming model; instead, it serves as a post-optimization uncertainty propagation tool for α,

where the posterior distribution provides a data-informed probabilistic weighting over parameter realizations applied to the already-optimized deterministic network. This design enables a direct comparison between Bayesian-informed cost uncertainty quantification and a uniform-distribution-based worst-case scenario analysis (i.e., α varying within ±30%), thereby providing decision-makers with both probabilistic cost estimates and conservative boundary evaluations under clearly stated assumptions.

5.1. Results of Bayesian and robust analyses

Table 12 summarizes the quantitative results of the deterministic baseline, Bayesian posterior analysis, and robust uniform analysis with α as the core parameter. Combined with the distribution characteristics in Figure 5, the results are interpreted from three perspectives: realism of expected cost, accuracy of uncertainty quantification, and decision-making value of risk premium.

Table 12. Quantitative analysis of CLSC network cost under recycling rate uncertainty.

Analysis Dimension	Baseline (α = 0.28)	Bayesian Posterior (Updated Belief)	Uniform Worst-Case (Max Entropy)
Panel A: Economic Metrics (Unit: Million CNY)			
Expected Total Cost	877.58	880.81	874.80
95% Uncertainty Width	—	11.83 (HDI)	108.02 (CI)
Diff. from Robust Cost	—	+6.02	—
Risk Premium*	—	7.89	—
Panel B: Parameter Configuration			
Recycling Rate (α)	Fixed Value	Concentrated	High Variance
Range Specification	0.28	0.27 ~ 0.29	0.196 ~ 0.364

* **Note:** The risk premium is defined as the difference between the upper bound of the 95% HDI from Bayesian analysis and the baseline value, representing the required budget buffer to mitigate underestimation risks.

From Table 12, several observations can be made: First, the discrepancy in expected cost stems from different distribution assumptions. The Bayesian posterior expected total cost reaches 880.81 million CNY, 6.02 million CNY higher than that under the robust scenario. A Beta$(3, 7)$ prior is adopted for the recycling rate α, with a mean of 0.30 close to the statutory target of 0.28. This prior is empirically specified based on MIIT regulatory data and EVTank (2024) industry surveys, which show that the formal recovery rate concentrates around the policy target with narrow variation. The prior confines α within 0.27–0.29, matching the moderate fluctuation feature of practical power battery recycling rates. MCMC sampling adopts 50,000 iterations with a 10,000-iteration burn-in period under standard empirical settings. By contrast, the robust analysis employs a uniform distribution over 0.196–0.364, covering extreme low-α cases and thus yielding a lower expected cost. Overall, the robust scenario reflects arbitrary parameter fluctuations without practical policy constraints, whereas the Bayesian approach produces cost estimates more consistent with industry reality.

Second, the disparity in interval width demonstrates the advantage of Bayesian methods in uncertainty quantification. The 95% highest density interval (HDI) in Bayesian analysis is only 11.83 million CNY, whereas the 95% confidence interval (CI) in robust analysis reaches 108.02 million CNY—approximately nine times wider. This illustrates the value of incorporating industry priors, which effectively suppress meaningless random perturbations and precisely define cost bounds under realistic α fluctuations. In contrast, robust analysis covers extreme, non-realistic scenarios, limiting its usefulness for refined budgeting.

Third, the risk premium metric enables quantitative decision-making. The Bayesian-derived risk premium is 7.89 million CNY, quantifying the minimum buffer needed to ensure network robustness under minor recycling rate fluctuations. Compared with the broad range from robust analysis, this premium aligns with practical needs for pre-allocating contingency funds, ensuring financial stability of the recycling network.

Moreover, Bayesian analysis shows that when α fluctuates within 0.27–0.29, the total network cost varies by only 1.35%, validating the effectiveness of the 1200-km reverse logistics constraint in the northwestern region. By expanding feasible reverse logistics zones from Urumqi and Xi'an, this constraint mitigates network contraction risk under α perturbations, ensuring CLSC cost robustness.

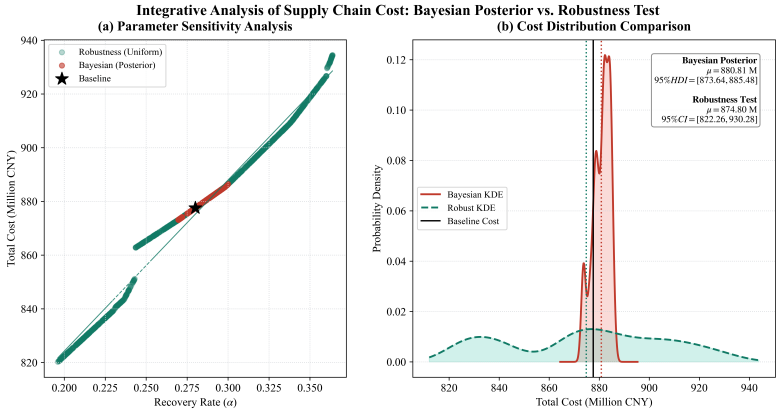

Figure 5. Integrated analysis of CLSC network cost under recycling rate α uncertainty. (a) Sensitivity of total cost to α: Bayesian posterior samples (red) cluster around the baseline value (black star, $\alpha = 0.28$), while robust samples (green) cover the full fluctuation range ($0.196 \sim 0.364$); (b) Cost distribution comparison: 95% HDI of Bayesian kernel density (red) is 11.83 million CNY, versus 95% CI of robust kernel density (green) at 108.02 million CNY, demonstrating the precision of Bayesian inference with the Beta prior compared to uniform assumption.

Figure 5 and empirical results further reveal two dimensions of academic value: parameter sensitivity and distribution characteristics.

As shown in Figure 5(a), total CLSC cost is strongly positively correlated with α, consistent with previous sensitivity analysis that identifies α as the key cost driver. Higher α increases reverse logistics flow and hub load, elevating system cost. Red Bayesian points cluster around the baseline, reflecting the Beta(3,7) prior guided, industry-consistent parameter distribution, while green robust points spread across the full range, representing uninformed fluctuation assumptions.

Figure 5(b) visualizes the uncertainty contrast. The Bayesian posterior exhibits a sharp-peaked, narrow-tailed distribution, indicating cost uncertainty is tightly controlled with prior information. The Robust distribution shows a flat, wide-tailed pattern, illustrating that uniform assumptions significantly amplify decision risk. This comparison validates Bayesian precision and highlights the critical role of northwestern differentiated logistics constraints in maintaining cost stability.

5.2. Managerial implications

Based on the empirical analysis, this study provides several managerial implications for planning and operating power battery recycling networks.

First, for budget formulation, CLSC planners should move beyond worst-case robust assumptions based on uniform distributions and adopt Bayesian decision-making with industry priors. Under the baseline scenario $\alpha = 0.28$, the network budget can be anchored at the Bayesian posterior mean cost of 880.81 million CNY, with an additional contingency reserve of 7.89 million CNY to hedge against moderate recycling-rate uncertainty. This approach translates uncertainty into an explicit and operationally interpretable budget buffer.

Second, reverse logistics planning should be spatially differentiated rather than governed by a uniform service radius. In sparsely populated northwestern areas (e.g., Urumqi, Lanzhou, and Xining), allowing a reverse logistics radius up to 1200 km preserves network accessibility without forcing underutilized local facilities. In densely populated central-eastern regions, the conventional 600-km radius remains sufficient to support cost-efficient clustered collection and transport. Such geographically tailored constraints mitigate the efficiency loss caused by overly stringent uniform requirements.

Third, investment priorities should emphasize forward logistics efficiency and hub capacity planning, rather than carbon penalty management. Under the baseline cost decomposition, forward logistics and fixed facility construction jointly account for nearly 90% of total system cost, whereas carbon-related costs contribute only 0.03%. When hub capacity is reduced below 68,000 units, the system is forced to deploy additional hubs, increasing fixed costs by approximately 4.56%. In contrast, expanding capacity beyond 104,000 units enables hub consolidation and yields cost savings of about 1.16%.

Fourth, recycling performance should be maintained within a stable operational interval. The Bayesian analysis identifies a robust range $\alpha \in [0.27, 0.29]$, within which total network cost varies by only 1.35%. Values below 0.27 may increase the risk of failing to meet statutory recovery obligations, while values above 0.29 lead to rapidly increasing marginal costs due to reverse logistics expansion and hub capacity saturation.

Finally, carbon pricing alone exerts limited structural impacts under the current cost framework. In the sensitivity experiments, a ±20% variation in the quota-plus-penalty amount alters the total cost by merely ±0.01% and exerts no material impact on optimal hub deployment or routing configuration. This indicates that standalone carbon pricing cannot drive structural low-carbon transformation of the supply chain. Complementary policy instruments, including targeted subsidies for green logistics, mandatory recycling requirements, and stricter enforcement of extended producer responsibility, are therefore necessary to deliver substantial emission abatement.

6. Conclusion

This study develops a CLSC network optimization model for power batteries, accounting for regional heterogeneity and demand uncertainty. By integrating Bayesian inference with worst-case scenario analysis, the model quantifies the impact of key parameter fluctuations on network configuration and operational performance. The main findings and managerial implications are summarized as follows.

First, we look at cost drivers and the limitations of environmental policies. Empirical results reveal that CLSC network costs are mainly driven by forward logistics expenditures and fixed facility investments, which jointly account for nearly 90% of the total cost. Under the current quota-plus-penalty and carbon allowance schemes, carbon-related costs contribute negligibly to overall system costs, standing at merely 0.03%. Sensitivity analysis further verifies that fluctuations in carbon pricing exert marginal impacts on core network configurations. This implies that relying solely on existing end-of-pipe carbon policies is insufficient to promote structural low-carbon transformation. Instead, firms should prioritize logistics route optimization and facility capacity utilization to reduce operational costs and improve system efficiency.

Second, we have risk quantification and budgetary guidance from a Bayesian perspective. Comparing Bayesian posterior analysis with uniform worst-case scenario analysis demonstrates the necessity of incorporating industry prior information. The worst-case analysis, which encompasses unrealistic extreme-low-recycling-rate scenarios, tends to underestimate expected costs. In contrast, Bayesian inference precisely characterizes the cost distribution when recycling rates fluctuate around policy targets, quantifying a risk premium of approximately 7.89 million CNY. This metric translates qualitative uncertainty descriptions into a quantitative budget buffer, and it is recommended that firms set network budgets based on the Bayesian high-density interval (HDI) rather than relying solely on deterministic estimates.

Third, we look at the value of spatial adaptation under regional heterogeneity constraints. The model validates the effectiveness of implementing a 1200-km differentiated reverse logistics radius for northwestern cities such as Urumqi and Xi'an. This strategy ensures network accessibility in remote areas while avoiding wasted fixed costs associated with underutilized facilities, achieving a synergistic balance between dense configuration in core regions and broad coverage in remote regions. Planners should therefore adopt geographically tailored logistics constraints instead of uniform distance limits to improve both network efficiency and resilience.

Finally, we consider threshold control of key operational parameters. The analysis identifies a statutory recycling rate of 0.28 and a recycling center capacity of 68,000 units as critical thresholds for network structural evolution. When actual parameters approach these thresholds, the network may experience structural shifts such as adjustments in facility count or rigid increases in core hub utilization. Consequently, managers should establish dynamic monitoring mechanisms to track fluctuations in recycling flows and core hub loads, rather than overreacting to minor carbon price changes, in order to maintain stable network operations during expansion phases.

Despite the contributions outlined above, this study has several limitations that warrant further investigation. The proposed network optimization model is formulated as a static single-period problem based on cross-sectional data from 2024–2025. Given the exponential growth trajectory of retired power batteries, extending the framework to a multi-period dynamic setting that captures

temporal demand evolution, dynamic battery retirement flows, and staged facility (or expansion) planning would provide more actionable guidance for long-term infrastructure planning. In addition, the current carbon regulation mechanism is simplified as a static quota-plus-penalty structure; future work could incorporate more realistic policy mechanisms, such as intertemporal quota banking and cross-enterprise trading. Furthermore, the current formulation assumes centralized decision-making, whereas real-world CLSC operations are typically governed by decentralized stakeholders with competing objectives. Incorporating strategic interactions through game-theoretic or bi-level optimization models could better reflect the behaviors of manufacturers, recyclers, and regulators. Furthermore, the model adopts a strategic-level flow abstraction rather than an operational mass-balance formulation. An explicit network balance constraint equating recycling center inputs and remanufactured outputs would require modeling yield coefficients and multi-product material flows, which is reserved for future research. These extensions represent promising directions for future research.

Author contributions

Weiwei Xu drafted the manuscript and assisted with figure preparation, while Lipu Zhang was responsible for model development and algorithm implementation.

Use of Generative-AI tools declaration

The authors declare no use of AI in this study.

Acknowledgments

This work is supported by the National Natural Science Foundation of China (Grant No. 61877053) and the Open Fund of Zhejiang Key Laboratory of Film and TV Media Technology (No. 2024E10023).

Supplementary

All the algorithm codes and figures used in this study are publicly available at the GitHub repository: https://github.com/locustzhang/Power-Battery-Closed-Loop-Supply-Chain-Optimization-under-Carbon-Tax-and-Demand-Uncertainty.

Conflict of interest

The authors have no competing interests to declare that are relevant to the content of this article.

References

1. A. M. Fathollahi-Fard, An integrated decision-making framework for a closed-loop supply chain network redesign problem, *AUIQ Tech. Eng. Sci.,* **1** (2024), 65–82. https://doi.org/10.70645/3078-3437.1016

2. A. M. Fathollahi-Fard, *Redesigning a closed-loop supply chain network in the tire industry,* Springer, 2025. https://doi.org/10.1007/978-3-032-00563-2-9
3. A. M. Fathollahi-Fard, Z. W. Li, Adaptive large neighborhood search algorithm for redesigning a closed-loop supply chain network considering capacity configurations, *Comput. Oper. Res.,* **190** (2026), 107415. https://doi.org/10.1016/j.cor.2026.107415
4. S. M. Ali, A. M. Fathollahi-Fard, R. Ahnaf, K. Y. Wong, A multi-objective closed-loop supply chain under uncertainty: An efficient Lagrangian relaxation reformulation using a neighborhood-based algorithm, *J. Clean. Prod.,* **423** (2023), 138702. https://doi.org/10.1016/j.jclepro.2023.138702
5. G. Alsanie, S. T. Unnisa, N. H. Al Hamad, Transforming the supply chain operations of electric vehicles' batteries using an optimization approach, *Sustainability,* **18** (2025), 367. https://doi.org/10.3390/su18010367
6. M. R. Khodoomi, B. M. Tosarkani, E. P. H. Li, Sustainable life cycle management of batteries in a closed-loop supply chain under hierarchical cost-sharing contracts and carbon policies, *Int. J. Prod. Econ.,* **290** (2025), 109799. https://doi.org/10.1016/j.ijpe.2025.109799
7. M. Zhang, I. S. Chang, J. Wu, Sustainability of lithium-ion battery recycling industry in China: An explorative analysis via an innovative dynamic business modeling for sustainability, *Energy,* **340** (2025), 139140. https://doi.org/10.1016/j.energy.2025.139140
8. X. Y. Gu, M. Y. Huang, L. Zhou, Reimagining government subsidy policies: facilitating echelon utilization and sustainable practices for retired battery systems, *Comput. Ind. Eng.,* **208** (2025), 111437. https://doi.org/10.1016/j.cie.2025.111437
9. N. Sihag, B. Vipin, Impact of policies on carbon and lead emissions in a closed loop lead–acid battery supply chain, *Clean. Logist. Supply Chain.,* **16** (2025), 100248. https://doi.org/10.1016/j.clscn.2025.100248
10. W. Q. Wu, M. Li, G. Q. Huang, Comparisons of government policies for electric automobile battery recycling using system dynamics, *Waste Manag.,* **203** (2025), 114892. https://doi.org/10.1016/j.wasman.2025.114892
11. W. Q. Wu, M. Li, M. Zhang, Y. Q. Wang, L. K. Wang, Y. You, Electric vehicle battery closed-loop supply chain pricing and carbon reduction decisions under the carbon cap-and-trade and reward-penalty policies, *Process Saf. Environ. Prot.,* **192** (2024), 1467–1482. https://doi.org/10.1016/j.psep.2024.10.121
12. Y. Qi, W. X. Yao, J. G. Zhu, Study on the selection of recycling strategies for the echelon utilization of electric vehicle batteries under the carbon trading policy, *Sustainability,* **16** (2024), 7737. https://doi.org/10.3390/su16177737
13. P. Narang, P. K. De, C. P. Lim, M. Kumari, Optimal recycling model selection in a closed-loop supply chain for electric vehicle batteries under carbon cap-trade and reward-penalty policies using the Stackelberg game, *Comput. Ind. Eng.,* **196** (2024), 110512. https://doi.org/10.1016/j.cie.2024.110512
14. C. Zhang, J. C. Li, Y. X. Tian, H. S. Li, Decisions on blockchain adoption and echelon utilization in the closed-loop supply chain for electric vehicles under carbon trading policy, *Inf. Sci.,* **681** (2024), 121247. https://doi.org/10.1016/j.ins.2024.121247
15. C. Zhang, Y. X. Chen, Y. X. Tian, Collection and recycling decisions for electric vehicle end-of-life power batteries in the context of carbon emissions reduction, *Comput. Ind. Eng.,* **175** (2023), 108869. https://doi.org/10.1016/j.cie.2022.108869

16. W. S. Zhang, T. Zhang, Recycling channel selection and financing strategy for capital-constrained retailers in a two-period, closed-loop supply chain, *Front. Environ. Sci.,* **10** (2022), 996009. https://doi.org/10.3389/fenvs.2022.996009
17. C. Zhang, Y. X. Tian, M. H. Han, Recycling mode selection and carbon emission reduction decisions for a multi-channel closed-loop supply chain of electric vehicle power battery under cap-and-trade policy, *J. Clean. Prod.,* **375** (2022), 134060. https://doi.org/10.1016/j.jclepro.2022.134060
18. N. Yao, F. Liu, Y. M. Zou, H. L. Wang, M. Zhang, X. Y. Tang, etal., Resuscitation of spent graphite anodes towards layer-stacked, mechanical-flexible, fast-charging electrodes, *Energy Storage Mater.,* **55** (2023), 417–425. https://doi.org/10.1016/j.ensm.2022.12.001
19. M. I. G. Salema, A. P. Barbosa-Póvoa, A. Q. Novais, A strategic and tactical model for closed-loop supply chains, *OR Spectr.,* **31** (2009), 573–599. https://doi.org/10.1007/s00291-008-0160-5
20. P. L. Zhang, L. Yang, L. Yin, Optimization design of closed-loop supply chain based on MILP model, *Int. Conf. Internet Comput. Inf. Serv.,* 2011, 103–106. https://doi.org/10.1109/ICICIS.2011.32
21. L. J. Zeballos, C. A. Méndez, A. P. Barbosa-Povoa, A. Q. Novais, Multi-period design and planning of closed-loop supply chains with uncertain supply and demand, *Comput. Chem. Eng.,* **66** (2014), 151–164. https://doi.org/10.1016/j.compchemeng.2014.02.027
22. F. Mohammed, A. Hassan, Optimal planning of a closed-loop supply chain with recovery options and carbon emission considerations, *IEEE Int. Conf. Ind. Eng. Eng. Manage.,* 2020, 54–58. https://doi.org/10.1109/IEEM45057.2020.9309835
23. J. Sun, Z. Chen, Z. Chen, X. Li, Robust optimization of a closed-loop supply chain network based on an improved genetic algorithm in an uncertain environment, *Comput. Ind. Eng.,* **189** (2024), 109997. https://doi.org/10.1016/j.cie.2024.109997
24. T. H. Hejazi, B. Khorshidvand, Robust optimization of sustainable closed-loop supply chain network considering product family, *Environ. Dev. Sustain.,* **26** (2024), 10591–10621. https://doi.org/10.1007/s10668-023-03166-4
25. S. Abbasi, B. Erdebilli, Green closed-loop supply chain networks' response to various carbon policies during COVID-19, *Sustainability,* **15** (2023), 3677. https://doi.org/10.3390/su15043677
26. M. Y. N. Attari, S. Rezanejad, A. Ala, V. Simic, D. Pamucar, Sustainable closed-loop supply chain network design under uncertainty using a fuzzy multi-objective optimization framework for the battery industry, *Sci. Rep.,* 2026. https://doi.org/10.1038/s41598-026-47477-8
27. S. Atti, H. Hassine, F. Djemal, S. Amari, *Designing a closed loop supply chain under carbon taxation policy,* Springer, 2025, 344–354. https://doi.org/10.1007/978-3-032-04742-7-35
28. S. Mitchell, M. O'Sullivan, I. Dunning, *PuLP: A linear programming toolkit for python,* New Zealand, 2011. Available from: https://github.com/coin-or/pulp
29. J. Forrest, R. Lougee-Heimer, *CBC User Guide, COIN-OR Foundation,* 2005. Available from: https://github.com/coin-or/Cbc

AIMS Press